Supporting Information

Two $\{Zn^{II}_2Dy^{III}\}$ complexes supported by monophenoxido/dicarboxylates bridges with multiple relaxation processes: carboxylato ancillary ligands controlled magnetic anisotropy in square antiprismatic Dy^{III} species

Min Li,[‡a] *Haipeng Wu*,[‡a] *Qing Wei*,*[a] *Hongshan Ke*,[a] *Bing Yin*,*[a] *Sheng Zhang*,[a,b] *Xingqiang Lv*,[b] *Gang Xie*[a] and *Sanping Chen**[a]

[a] Key Laboratory of Synthetic and Natural Functional Molecule Chemistry of Ministry of Education, College of Chemistry and Materials Science, Key Laboratory of Synthetic and Natural Functional Molecule Chemistry of Ministry of Education, College of Chemistry and Materials Science, Northwest University, Xi'an, 710127, China.

[b] School of Chemical Engineering, Northwest University, Xi'an, 710127, China.

Email: Weiqq@126.com; rayinyin@nwu.edu.cn; sanpingchen@126.com

[‡] These authors contributed equally to this work.

***Corresponding authors**

Prof. Qing Wei

E-mail: weiqq@126.com

Prof. Bing Yin

E-mail: rayinyin@nwu.edu.cn

Prof. Sanping Chen

E-mail: sanpingchen@126.com

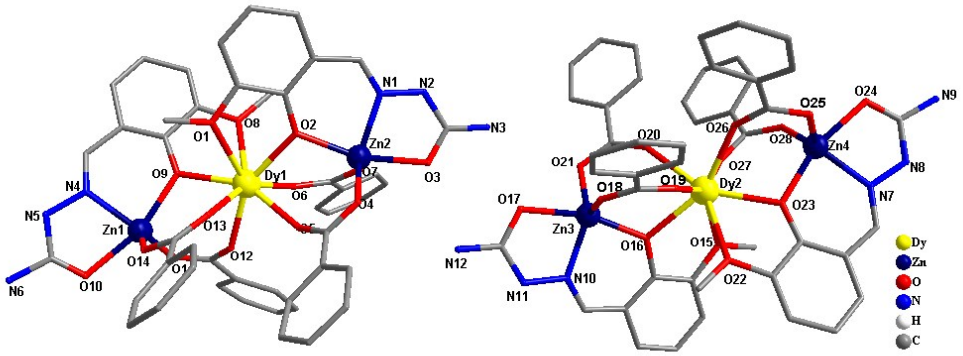

Figure S1. Dy1 and Dy2 enantiomers of complex **1**.

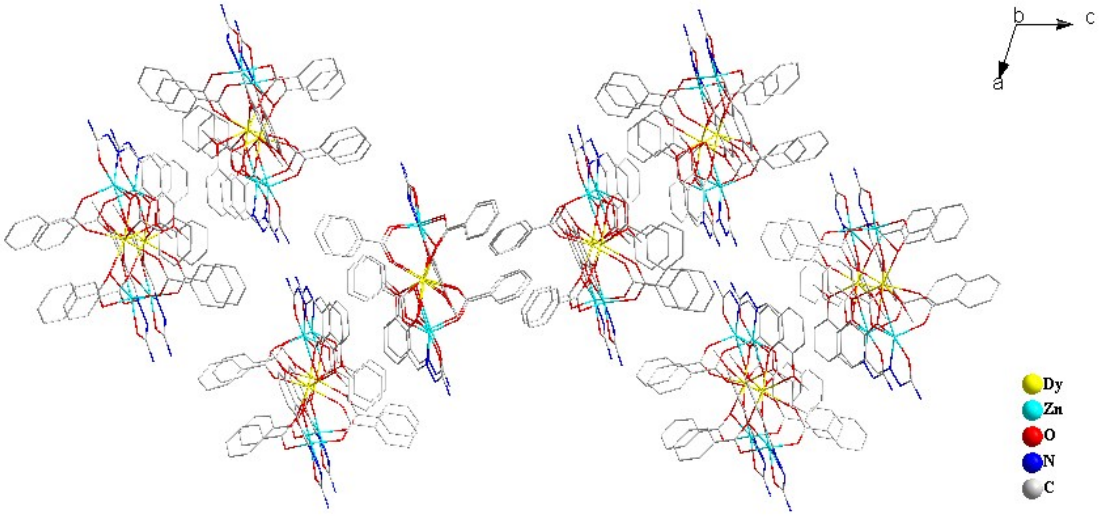

Figure S2. The packing diagrams along crystallographic axes for **1**.

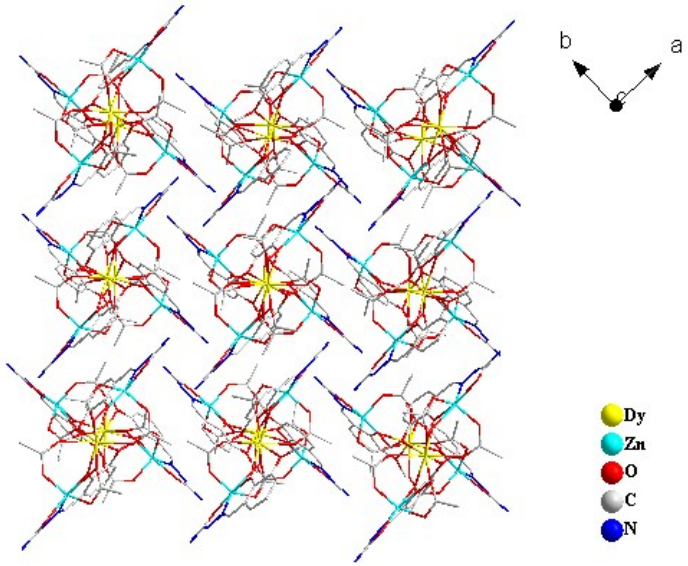

Figure S3. The packing diagrams along crystallographic axes for **2**.

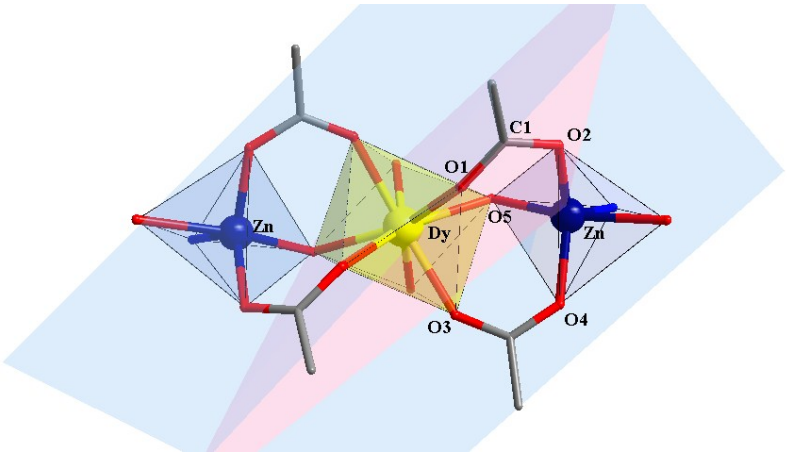

Figure S4. The schematic diagram of distortion of carboxylate groups and a stretched Dy-$O_{phenoxo}$ distance of **1** and **2**. Large dihedral angle composed by Dy-O1-C1 and C1-O2-Zn are to be 63.627°, 65.626°, 71.776° and 63.744° in **1**a, **1**b, **2**a and **2**b, respectively (**2**a and **2**b are two disordered structures of complex **2**).

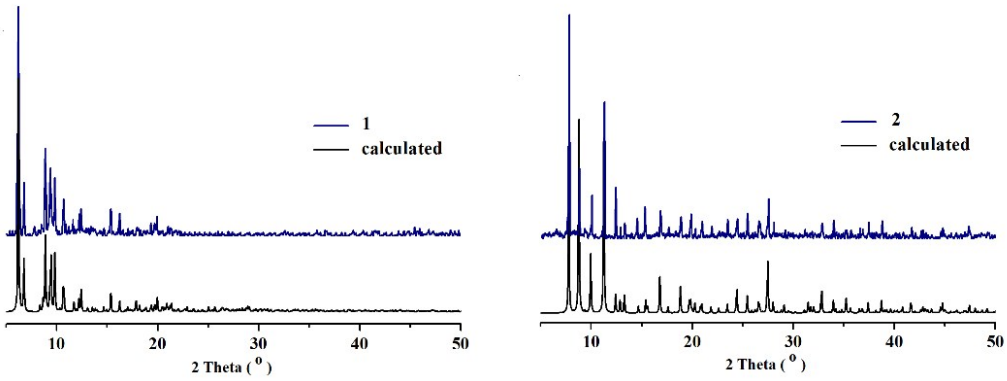

Figure S5. PXRD curves for **1-2**.

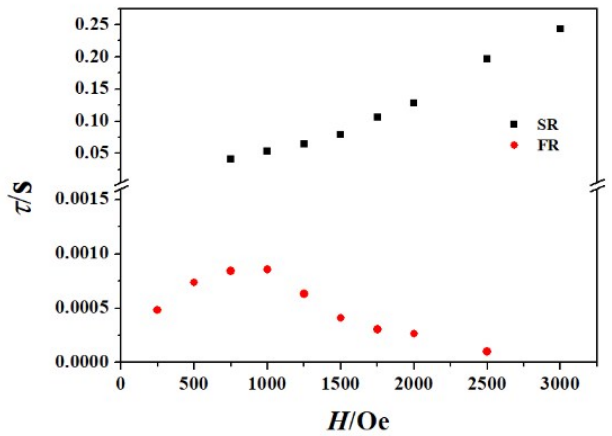

Figure S6. Field dependence of the magnetic relaxation time at 2 K for two relaxation processes

(SR and FR) of complex **1**.

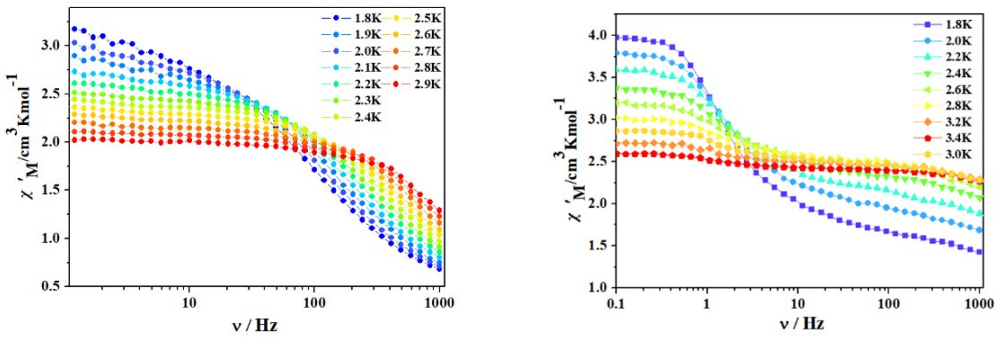

Figure S7. Field dependence of the in-phase signal (χ') under (a) 500 Oe and (b) 2000Oe dc field for **1**.

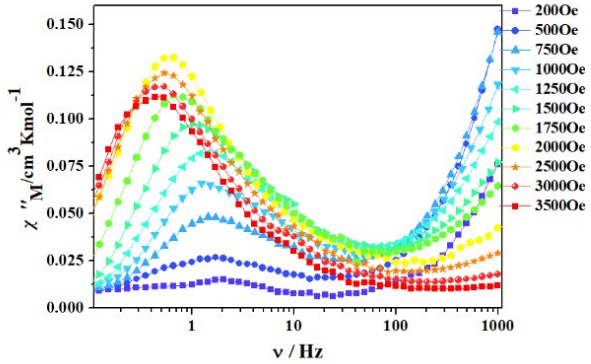

Figure S8. Field dependence of the out-of-phase signal *vs* frequency at 2 K for **2**.

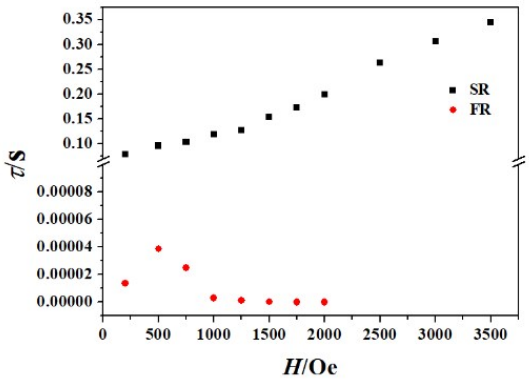

Figure S9. Field dependence of the magnetic relaxation time at 2 K for two relaxation processes (SR and FR) of complex **2**.

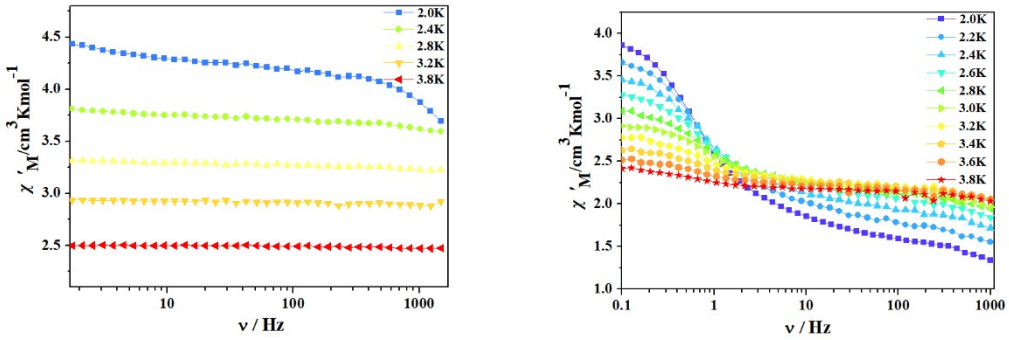

Figure S10. Field dependence of the in-phase signal (χ') under (a) 500 Oe and (b) 2000Oe dc field for **2**.

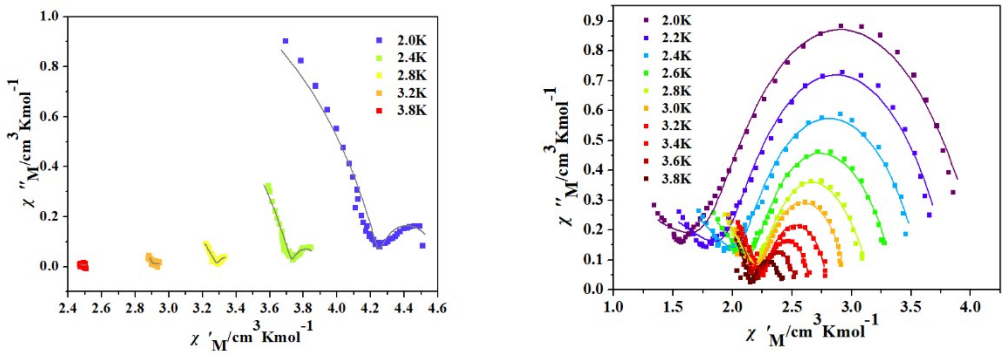

Figure S11. Cole-Cole plots under (a) 500 Oe and (b) 2000Oe dc field for **2**. Solid lines in Cole-Cole plots are fitting results by the sum of two modified Debye functions.

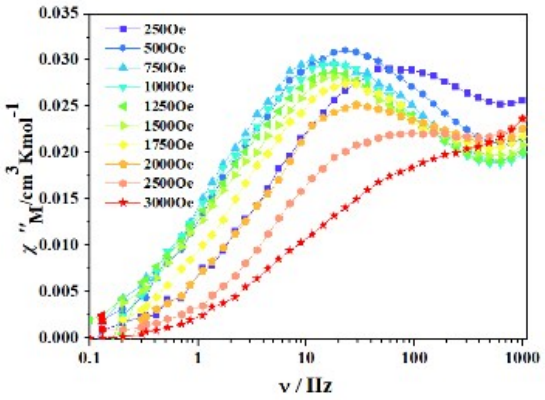

Figure S12. Field dependence of the out-of-phase signal *vs* frequency at 2 K for **1'**.

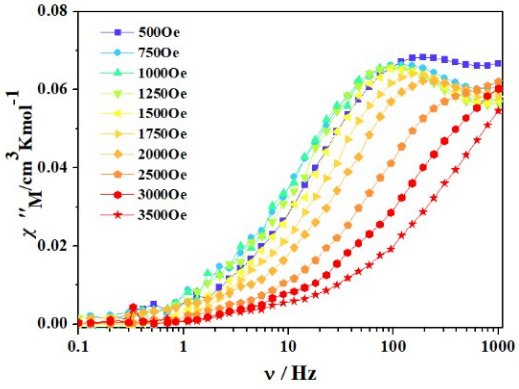

Figure S13. Field dependence of the out-of-phase signal *vs* frequency at 2 K for **2'**.

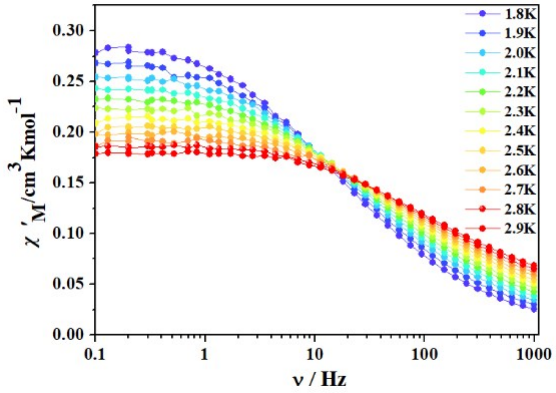

Figure S14. Field dependence of the in-phase signal (χ') under 500 Oe dc field for **1'**.

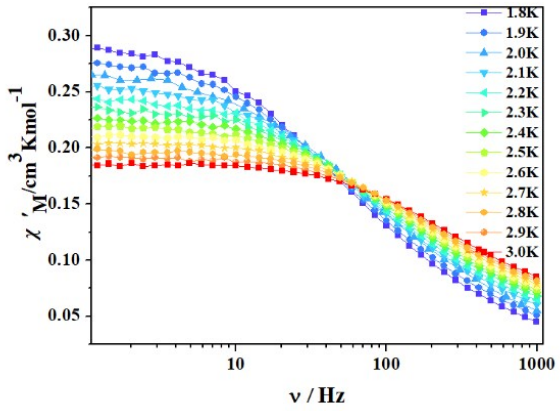

Figure S15. Field dependence of the in-phase signal (χ') under 500 Oe dc field for **2'**.

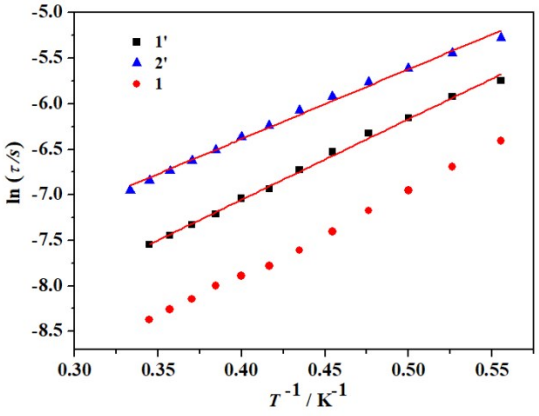

Figure S16. The Arrhenius plots under the optimized dc field for **1'** and **2'**. The solid lines represent the fitting with the Arrhenius law.

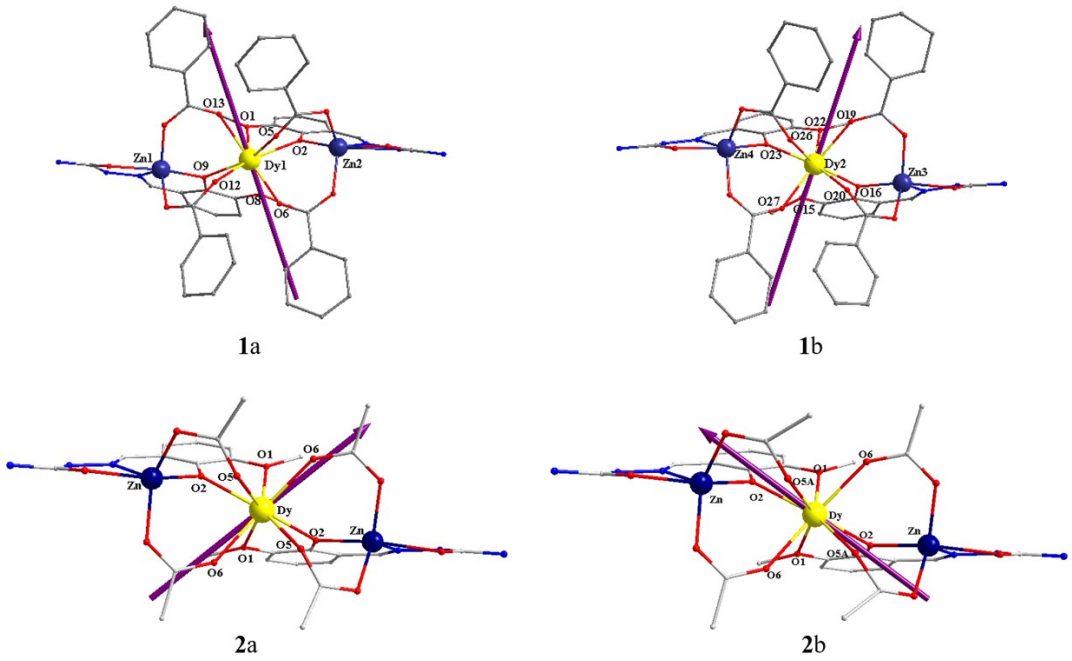

Figure S17. Direction of the *ab initio* magnetic easy axis of the ground KDs of the two possible geometry configurations of complexes **1** and **2**.

Table S1. Crystal data and structure refinement summary for complexes **1** and **2**.

	1	**2**
Empirical formula	$C_{106}H_{90}Dy_2N_{12}O_{32}Zn_4$	$C_{30}H_{38}N_6O_{18}DyZn_2$
Formula weight	2630.37	1063.90
Crystal system	Monoclinic	Tetragonal
Space group	$P2_1$	$P4_2/n$
a (Å)	21.333(5)	14.2398(17)
b (Å)	10.771(2)	14.2398(17)
c (Å)	27.313(6)	18.844(2)
α (°)	90	90
β (°)	106.737(4)	90
γ(°)	90	90
V (Å^3)	6010(2)	3820.9(10)
Z	2	4
D_c (g m^{-3})	1.454	1.849
μ (mm^{-1})	2.090	3.265
F (000)	2636.0	2120.0
Reflns collected/unique	30261 / 20328	22174/ 4412
R_{int}	0.0525	0.0548
GOF on F^2	0.944	1.018
R_1[a] [$I > 2\sigma(I)$]	0.0581	0.0552
wR_2[b] (all data)	0.1344	0.1966
Flack factor	0.025(18)	
CCDC	1818259	1818260

[a] $R_1 = \Sigma(||F_o| - |F_c||)/\Sigma|F_o|$. [b] $wR_2 = [\Sigma w(F_o^2 - F_c^2)^2/\Sigma w(F_o^2)^2]^{1/2}$.

Table S2. Selected bond distance (Å) and bond angle (°) for **1** and **2**.

Complex **1**			
Dy1-O9	2.346(10)	O9-Dy1-O1	75.6(4)
Dy1-O12	2.322(11)	O9-Dy1-O8	64.8(4)
Dy1-O1	2.524(11)	O12-Dy1-O9	76.2(4)
Dy1-O2	2.346(10)	O12-Dy1-O1	141.9(4)
Dy1-O6	2.280(11)	O12-Dy1-O2	152.5(4)
Dy1-O13	2.267(12)	O12-Dy1-O8	117.0(4)
Dy1-O5	2.296(12)	O2-Dy1-O9	130.2(4)
Dy1-O8	2.494(12)	O2-Dy1-O1	63.4(4)
Dy2-O25	2.272(11)	O2-Dy1-O8	76.1(4)
Dy2-O22	2.312(12)	O6-Dy1-O9	109.3(4)
Dy2-O19	2.347(11)	O6-Dy1-O12	78.5(4)
Dy2-O18	2.505(11)	O6-Dy1-O1	135.4(4)
Dy2-O23	2.285(12)	O6-Dy1-O2	84.1(4)
Dy2-O16	2.367(10)	O6-Dy1-O5	81.0(4)
Dy2-O27	2.324(11)	O6-Dy1-O8	71.1(4)

Dy2-O15	2.504(12)	O13-Dy1-O9	84.1(4)
Zn3-O21	1.994(11)	O13-Dy1-O12	81.7(4)
Zn3-O24	1.939(12)	O13-Dy1-O1	70.4(4)
Zn3-O17	2.104(13)	O13-Dy1-O2	106.0(4)
Zn3-O16	2.067(12)	O13-Dy1-O6	152.4(4)
Zn3-N10	2.067(14)	O13-Dy1-O5	76.5(5)
Zn1-O9	2.116(11)	O13-Dy1-O8	135.9(4)
Zn1-N4	2.081(14)	O5-Dy1-O9	150.5(4)
Zn1-O14	1.939(11)	O5-Dy1-O12	79.1(4)
Zn1-O10	2.175(11)	O5-Dy1-O1	117.1(4)
Zn1-O11	1.950(11)	O5-Dy1-O2	77.2(4)
Zn2-O3	2.159(12)	O5-Dy1-O8	142.9(4)
Zn2-O2	2.077(11)	O8-Dy1-O1	72.0(4)
Zn2-O4	1.968(12)	O25-Dy2-O22	78.0(4)
Zn2-O7	1.946(12)	O25-Dy2-O19	82.8(4)
Zn2-N1	2.062(15)	O25-Dy2-O18	135.5(4)
Zn4-O19	2.104(12)	O25-Dy2-O23	152.7(4)
Zn4-O28	1.968(12)	O25-Dy2-O16	106.5(4)
Zn4-O26	1.936(14)	O25-Dy2-O27	82.5(4)
Zn4-N7	2.054(17)	O25-Dy2-O15	69.7(4)
Zn4-O20	2.137(14)	O22-Dy2-O19	152.0(4)
O19-Dy2-O15	73.7(4)	O22-Dy2-O18	141.4(4)
O23-Dy2-O22	80.6(4)	O22-Dy2-O16	74.7(4)
O23-Dy2-O19	110.1(4)	O22-Dy2-O27	82.2(4)
O23-Dy2-O18	70.9(4)	O22-Dy2-O15	117.2(4)
O23-Dy2-O16	83.7(4)	O19-Dy2-O18	65.2(4)
O23-Dy2-O27	78.0(4)	O19-Dy2-O16	130.8(4)
O23-Dy2-O15	136.2(4)	O16-Dy2-O18	76.8(4)
O16-Dy2-O15	65.5(4)	O27-Dy2-O16	152.6(4)
O27-Dy2-O19	75.3(4)	O27-Dy2-O15	140.4(4)
O27-Dy2-O18	115.4(4)	O15-Dy2-O18	72.1(4)

Complex **2**

Dy1-O2	2.318(5)	O6-Dy1-O6^{1}	156.5(3)
Dy1-O2^{1}	2.318(5)	O5^{1}-Dy1-O2^{1}	75.3(3)
Dy1-O1	2.532(5)	O5^{1}-Dy1-O2	148.1(3)
Dy1-O1^{1}	2.531(5)	O5-Dy1-O2^{1}	148.1(3)
Dy1-O6	2.305(6)	O5-Dy1-O2	75.3(3)
Dy1-O6^{1}	2.305(6)	O5-Dy1-O1	118.8(5)
Dy1-O5^{1}	2.294(7)	O5^{1}-Dy1-O1^{1}	118.8(5)

Dy1-O5	2.294(7)	O5-Dy1-O1^{1}	144.5(5)
Dy1-O5A^{1}	2.285(15)	O5^{1}-Dy1-O1	144.5(5)
Dy1-O5A	2.285(15)	O5^{1}-Dy1-O6^{1}	81.6(6)
Zn1-O2	2.104(5)	O5-Dy1-O6	81.6(6)
Zn1-O3	2.185(5)	O5-Dy1-O6^{1}	79.9(6)
Zn1-O7	1.952(6)	O5^{1}-Dy1-O6	79.9(6)
Zn1-N1	2.073(7)	O5-Dy1-O5^{1}	76.5(6)
Zn1-O4	1.983(8)	O5A^{1}-Dy1-O2	144.7(9)
Zn1-O4A	1.977(15)	O5A^{1}-Dy1-O2^{1}	74.7(8)
O2-Dy1-O2^{1}	135.6(2)	O5A-Dy1-O2^{1}	144.7(9)
O2-Dy1-O1	64.71(18)	O5A-Dy1-O2	74.7(8)
O2^{1}-Dy1-O1^{1}	64.71(18)	O5A^{1}-Dy1-O1	150.6(9)
O2^{1}-Dy1-O1	78.67(18)	O5A-Dy1-O1^{1}	150.6(9)
O2-Dy1-O1^{1}	78.67(18)	O5A^{1}-Dy1-O1^{1}	109.5(11)
O1^{1}-Dy1-O1	68.9(3)	O5A-Dy1-O1	109.5(11)
O6-Dy1-O2^{1}	107.5(2)	O5A^{1}-Dy1-O6	69.8(11)
O6^{1}-Dy1-O2	107.5(2)	O5A^{1}-Dy1-O6^{1}	92.7(12)
O6^{1}-Dy1-O2^{1}	81.59(19)	O5A-Dy1-O6^{1}	69.8(11)
O6-Dy1-O2	81.60(19)	O5A-Dy1-O6	92.7(12)
O6-Dy1-O1	131.4(2)	O5A-Dy1-O5A^{1}	86.1(19)
O6-Dy1-O1^{1}	71.0(2)	O6^{1}-Dy1-O1^{1}	131.4(2)
O6^{1}-Dy1-O1	71.0(2)		

Symmetry transformations used to generate equivalent atoms:

^{1}1/2-X,3/2-Y,+Z

Table S3. Shape analysis for the metal centers of **1.**

ML8	SAPR-8	TDD-8	JSD-8	JBTPR-8	BTPR-8
Dy1	**0.674**	1.892	3.972	2.310	2.029
Dy2	**0.598**	1.827	4.178	2.398	1.945

Table S4. Shape analysis for the metal centers of **2.**

ML8	SAPR-8	TDD-8	JSD-8	JBTPR-8	BTPR-8
Dy1	**0.768**	2.207	3.869	3.869	2.152

SAPR-8 (D_{4d}): Square antiprism

TDD-8 (D_{2d}): Triangular dodecahedron

JSD-8 (D_{2d}): Snub diphenoid J84

JBTPR-8 (C_{2v}): Biaugmented trigonal prism J50

BTPR-8 (C_{2v}): Biaugmented trigonal prism

Table S5. *Ab initio* computed relative energies (in cm^{-1}), principal values of the g-tensors and averaged transition magnetic moment μ_{QTM} (in β) of the four lowest KDs of the complexes studied in this work.

		1a	**1**b	**2**a	**2**b
KD_0	E	0.00	0.00	0.00	0.00
	g_Z	18.342	19.058	18.678	17.879
	g_X	0.514	0.306	0.865	0.010
	g_Y	1.504	0.861	1.499	0.384
	g_{XY}	1.590	0.914	1.731	0.384
	g_{XY}/g_Z	0.087	0.047	0.093	0.021
	μ_{QTM}	0.337	0.195	0.394	0.066
KD_1	E	35.5	61.2	32.1	47.1
	g_Z	14.692	13.920	13.617	17.589
	g_X	1.359	1.279	1.336	0.809
	g_Y	3.269	2.302	2.619	0.869
	g_{XY}	3.541	2.633	2.940	1.187
	g_{XY}/g_Z	0.241	0.189	0.216	0.068
	μ_{QTM}	0.772	0.597	0.659	0.280
KD_2	E	79.8	101.5	74.7	78.5
	g_Z	11.691	13.394	13.039	9.403
	g_X	0.430	0.156	0.506	4.158
	g_Y	1.602	2.977	1.381	6.232
	g_{XY}	1.659	2.981	1.471	7.491
	g_{XY}/g_Z	0.142	0.223	0.113	0.797
	μ_{QTM}	0.339	0.522	0.315	1.732
KD_3	E	98.1	121.0	92.0	88.5
	g_Z	11.399	2.865	10.151	0.319
	g_X	2.659	5.652	1.009	11.970
	g_Y	4.360	5.213	2.530	6.734
	g_{XY}	5.107	7.689	2.724	13.740
	g_{XY}/g_Z	0.448	2.683	0.268	43.070
	μ_{QTM}	1.170	1.811	0.590	3.118

Table S6. The negative charges of the O atoms in the first sphere (in |e|) from *ab initio* calculations and the related Dy-O bond lengths (in Å)[a]

1a	O_6-ax	O_{13}-ax	O_2-Zn	O_9-Zn	O_5-car	O_{12}-car	O_1-alk	O_8-alk
Charge	0.759	0.731	0.869	0.850	0.780	0.778	0.428	0.445
Dy-O	2.293	2.286	2.348	2.342	2.308	2.341	2.555	2.506
θ[b]	12.67	14.86						
1b	O_{19}-ax	O_{27}-ax	O_{16}-Zn	O_{23}-Zn	O_{20}-car	O_{26}-car	O_{15}-alk	O_{22}-alk
Charge	0.762	0.796	0.903	0.851	0.772	0.748	0.452	0.442
Dy-O	2.281	2.270	2.366	2.347	2.286	2.304	2.472	2.493
θ	8.09	19.76						
2a	O_6-ax	O_6-ax	O_2-Zn	O_2-Zn	O_5-car	O_5-car	O_1-alk	O_1-alk
Charge	0.766	0.766	0.872	0.872	0.762	0.762	0.443	0.443
Dy-O	2.305	2.305	2.318	2.318	2.294	2.294	2.532	2.532

θ	14.35							
2b	O_2-ax	O_2-ax	O_6-car	O_6-car	O_{5A}-car	O_{5A}-car	O_1-alk	O_1-alk
Charge	0.864	0.864	0.761	0.761	0.815	0.815	0.441	0.441
Dy-O	2.356	2.356	2.294	2.294	2.285	2.285	2.532	2.532
θ	23.85							

[a] "-ax" means the O atoms at the axial position, "-Zn" means the O atoms connected with Zn atom, "-car" means the O atoms from the carboxy group, "-alk" means the alkoxy O atoms. b the angle between the magnetic easy axis and a given Dy-O bond (in ◦)